Chemical and Thermodynamic Control of the Surface of Semiconductor Nanocrystals for Designer White Light Emitters

Michael M. Krause, Jonathan Mooney, and Patanjali Kambhampati*

Department of Chemistry, McGill University, Montreal, QC, H3A 3R8, Canada

ABSTRACT Small CdSe semiconductor nanocrystals with diameters below 2 nm are thought to emit white light due to random surface defects which result in a broad distribution of midgap emitting states, thereby preventing rational design of small nanocrystal white light emitters. We perform temperature dependent photoluminescence experiments before and after ligand exchange and electron transfer simulations to reveal a very simple microscopic picture of the origin of the white light. These experiments and simulations reveal that these small nanocrystals can be physically modeled in precisely the same way as normal-sized semiconductor nanocrystals; differences in their emission spectra arise from their surface thermodynamics. The white light emission is thus a consequence of the thermodynamic relationship between a core excitonic state and an optically bright surface state with good quantum yield. By virtue of this understanding of the surface and the manner in which it is coupled to the core excitonic states of these nanocrystals, we show both chemical and thermodynamic control of the photoluminescence spectra. We find that using both temperature and appropriate choice in ligands, one can rationally control the spectra so as to engineer the surface to target color rendering coordinates for displays and white light emitters.

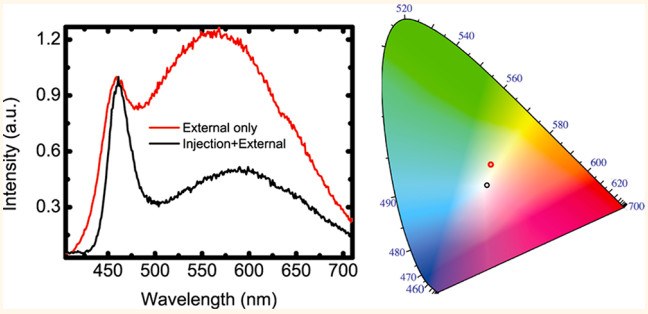

KEYWORDS: nanocrystal · quantum dots surface emission · surface traps · white light emission · temperature-dependence · CIE-coordinates

Illumination accounts for 20% of the world's energy consumption. In the next two decades, electricity consumption for lighting alone is expected to rise by 60%.[1] To sustain and ease this development increasing focus is being placed on the development of sustainable, energy efficient lighting solutions, for example, white light creation *via* light emitting diodes (LEDs).

Semiconductor nanocrystals (NCs) have been the focus of extensive interest due to their unique optical and electronic properties.[2−4] These nanostructures have well-studied size tunable optical properties, and are known to display high quantum yields,[5] simple solution phase processability, and good photochemical stability. Following the seminal work of Bawendi and Bulovic,[6] a wide variety of NC-based LEDs have been developed.[3,7,8] In some display applications, a critical figure of merit of an eye pleasing light source is a broad and well-balanced spectrum as benchmarked by the Commission Internationale de l'Éclairage (CIE) coordinates. The CIE coordinates give information on the color sensation perceived by an observer when looking at a light source. It ranges throughout the visible spectrum and at its center displays a region that is perceived as white light by an average human observer.

There are a few primary approaches toward creating broad emission spectra with target CIE coordinates using semiconductor nanocrystals as an active element. The first approach is to produce a white light spectrum by mixing NCs of different emission color.[9] However, multilayered devices created in this manner are susceptible to efficiency loss due to self-absorption.[10] Another approach is to synthesize multishell NCs that emit a white light spectrum from the

* Address correspondence to pat.kambhampati@mcgill.ca.

Received for review March 19, 2013 and accepted June 26, 2013.

Published online June 26, 2013
10.1021/nn401383t

© 2013 American Chemical Society

combination of different colored light from distinct shells.[4] This approach results in NCs with high photoluminescence (PL) quantum yields, but requires a complicated multistep synthesis. A third approach is to create very small CdSe NCs that have both some distribution of band edge excitonic (core) PL and a broad deep trap (surface) PL.[2] The benefit of this approach is that it only requires a simple single step synthesis. As the nature of the interplay of core and surface PL leading to white light emission is poorly understood, however, this method of white light creation has been described as taking place "by chance"[4] due to ill-defined surface defects as the source.

Here, we report on temperature-dependent photoluminescence (PL) spectroscopy on small CdSe NCs with various surface chemistries so as to identify the microscopic mechanism by which white light emission from nanocrystals may be engineered and rationally controlled. CdSe NCs were synthesized following the work of Peng and Peng[11] with slight modifications. Previously, Rosenthal argued that these small NCs emit white light at room temperature due to a presumed broad distribution of surface defects.[2] We find that ligand exchange from phosphines to amines and choice of temperature dramatically alter the relative amounts of surface *versus* band edge excitonic PL. We show that these results can be fully explained using a semiclassical electron transfer model recently introduced for surface trapping in normal-sized II–VI semiconductor nanocrystals.[12] We recently published a revised version of the model that explicitly accounts for nonradiative processes from the surface, which is used to fit the data shown.[13]

Our findings suggest that ligand passivation controls the thermodynamics of excitonic population in equilibrium between the band edge exciton and the surface of the nanocrystal. In addition we show that ultrasmall NCs can be explained as a subset of "normal-sized" NCs. We find, in contrast to previous suggestions,[2] that high quality white light performance can be achieved in single emitter NCs though a good balance between core and surface populations. These experiments and simulations suggest that both surface chemistry and temperature may be exploited to control the relative populations of core and surface states. This excitonic population control *via* surface chemistry therefore enables control of the CIE coordinates, a key step toward effective use of these NCs in displays and lighting applications.

RESULTS AND DISCUSSION

Figure 1 shows absorption and PL spectra of small CdSe NCs synthesized with trioctylphosphine oxide (TOPO) ligands both before and after postsynthetic ligand exchange to butylamine. The absorption spectra (Figure 1a) shows the lowest absorption features (band edge exciton) at 2.87 eV for TOPO capped NCs

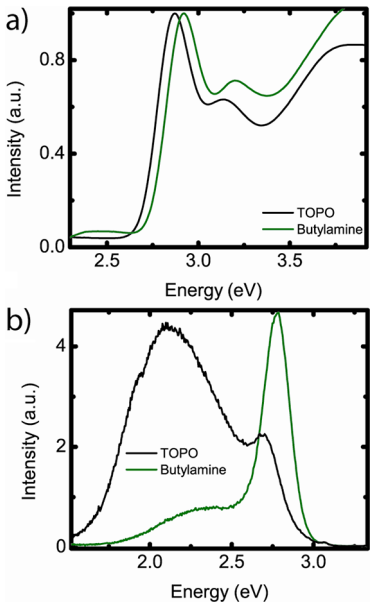

Figure 1. Room temperature absorption and photoluminescence (PL) spectra of the TOPO passivated NCs, before (TOPO) and after ligand exchange with butylamine. (a) The first absorption feature (band edge exciton) shifts from 2.87 to 2.92 eV, suggesting a small change in crystal size upon ligand exchange. (b) The PL spectra show considerable difference, however. The samples were excited at 360 nm, the plots were normalized by the absorbance at excitation wavelength. The second order diffraction of the grating in the PL spectrometer at ~1.72 eV was removed in the data processing stage.

and at 2.92 eV for butylamine capped NCs. As the energy of this absorption feature is directly related to the quantum confinement of the exciton within the nanocrystal, one can determine the size of the nanocrystal from the energy of the absorption feature.[14] From the energy of the first absorption feature it is estimated that the NCs both have a diameter of ~1.8 nm, before and after the ligand exchange.[14]

The blueshifting of the band edge exciton (Figure 1a) can be explained by either an edging of the NCs caused by some surface atoms being stripped from the crystal by leaving TOPO molecules,[15,16] or by a redistribution of electronic density of the NC core.[5] To determine the reason for this shift, a ligand exchange from butylamine back to TOPO was performed.[5] Since the absorption feature did not shift back to the original position, but further to the blue, we conclude the shifting is caused by edging of the NC surface atoms caused by the ligand exchange reaction. Other than this small blueshifting as expected from a ligand exchange, the spectral features in the absorption spectra are largely unchanged. Hence the ligand exchange can be considered to preserve the electronic structure of the CdSe core excitonic states.

Figure 1b shows the PL spectra of the TOPO and butylamine capped NCs. Both samples were excited at 360 nm (3.44 eV) and the spectra were normalized to their absorbance at this wavelength in order for the

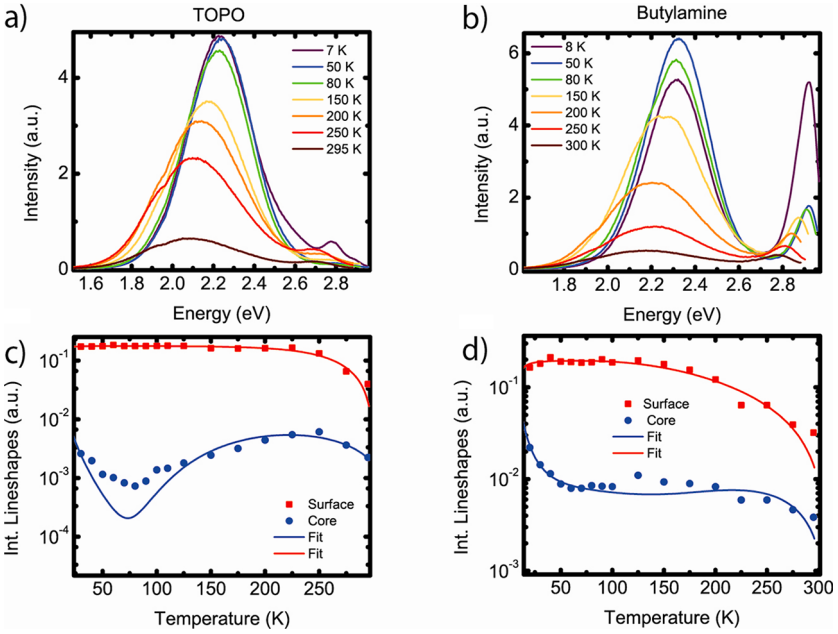

Figure 2. Surface passivation dictates the thermodynamics of the PL spectra. (a) PL spectra upon excitation of the TOPO passivated NCs resonant with the band edge exciton. Only selected spectra are shown for clarity (b) Same as in panel a, upon excitation of the butylamine passivated NCs. (c) The integrated spectral lineshapes (see text for details) *vs* temperature. (d) Same as in panel c, for the butylamine passivated NCs. Points are data and lines are fits to a semiclassical electron transfer surface trapping model (see text for details).

intensities to reflect the relative quantum yields. Both spectra exhibit two distinct PL peaks. The more defined peak at higher energy (2.70 eV for TOPO capped NCs, 2.78 eV for butylamine capped NCs) is due to PL from the core band edge exciton, whose electronic structure is now well understood. The surface band is red-shifted from the core band. This surface PL band is thought to arise from a distribution of nonpassivated selenium defects on the nanocrystal surface.[17,18]

While the absorption spectra for the differently capped NCs are very similar, there are large differences between the PL spectra. The majority of the radiation for the TOPO passivated NCs comes from the surface, and the spectrum is very broad (with fwhm of ~0.6 eV). In the case of the butylamine passivated NCs the core radiation is enhanced by 68% and the surface radiation is substantially quenched. This result indicates that by chemically manipulating the surface of a nanocrystal one can not only quench emission, but enhance specific radiative pathways.

To understand the spectral outcomes for differently passivated NCs one has to take a closer look at the ligand passivation process. Amine ligands have been known to increase the PL quantum yield of NCs relative to TOPO passivation.[5] Previous work has suggested that poor surface passivation is the cause of nonradiative relaxation pathways, which decrease the quantum yield.[16,19] Since butylamine binds strongly to the NC surface and is less sterically hindered than TOPO, higher capping densities are achieved.[20] Previous work by Landes *et al*. has also shown that exchanging TOPO with butylamine ligands on small NCs can quench surface radiation without enhancement of the core emission,[21] which strongly differs from the results presented in this paper (shown in Figure 1b). The discrepancy could be explained by the fact that in our ligand exchange reaction the NCs were neatly dissolved in butylamine, as compared to simply adding butylamine to a nanocrystal/toluene solution. Our procedure allows a much higher concentration of butylamine ligands in the reaction, so a more complete passivation is likely.

Figure 2 shows the temperature-dependent PL spectra of the two NCs of different passivation. In both systems, the surface band monotonically increases in intensity as temperature is lowered, ultimately saturating at some maximum value. This response is entirely consistent with the behavior of the band edge exciton in any number of NC systems. In contrast, the PL response of the band edge exciton here is quite complex. In the case of the TOPO passivated NCs, the core PL initially increases as temperature is lowered, precisely as expected. Remarkably, the core PL then *decreases* in intensity by an order of magnitude as temperature is lowered from 250 to 70 K, only to increase again as the NCs is further cooled to below 50 K. Butylamine-capped NCs display a similar trend for the surface emission. However, the core radiation peak intensity never decreases to the noise level and can be observed throughout the temperature range of the experiment. The blueshift and narrowing of the core and surface PL bands with decreasing temperatures is consistent with prior work.[12,21]

Figure 2 panels c and d show the integrated intensities of the core radiation and surface PL bands at

different temperatures, for TOPO passivated and butylamine passivated NCs. Before integration the spectra were converted into spectral lineshapes to factor out the ν^3 dependence to spontaneous emission, to give a better representation of the actual carrier populations that lead to core and surface radiation.[12]

The data clearly show a thermodynamic relation of the two distinct bands. Traditionally, the surface radiation had been thought to arise from a broad distribution of midbandgap deep trap states,[12,22,23] but this approach does not account for the temperature dependence of the surface quantum yield. We recently presented a semiclassical electron transfer (ET) model for surface trapping in semiconductor nanocrystals which accounts for the temperature dependent changes in the ratio of core and surface radiation.[12] In classical electron transfer theory, internal configurational changes are disregarded and only low-frequency modes representing interaction with the medium are considered.[24] This approach has been shown to not adequately account for electron transfer rates over the entire temperature regime in several systems.[24] Here, we invoke a semiclassical electron transfer approach to surface trapping in which the vibrational modes are modeled by partitioning into a single mean high-frequency mode representing internal configurational changes and a single mean low-frequency mode representing interactions with the medium/ligands.

In our system, a single core excitonic state (band edge exciton) is coupled to a single surface state *via* these modes. The classical mode corresponds to interactions involving the ligand and the bath, whereas the quantum mode corresponds to the longitudinal optical (LO) phonon internal to the NCs. Tunneling through the potential barrier is allowed *via* this quantum mode, a significant point in determining ET behavior at low temperature which is neglected in classical ET theory. For the classical mode, a small free energy difference ΔG and activation barrier ΔG^* (Figure 3a) between the 1S band edge exciton and the surface state dictates the thermodynamics of the populations. In ET-theory, this activation barrier ΔG^* emerges mathematically from the free energy difference ΔG and the reorganization energy λ_{medium}, a parameter representing the energy difference between the two parabolic free energy surfaces at any given configuration coordinate (Figure 3a). However, the quantum mode, in which vibrational energy levels are larger than thermal energy, is singularly characterized by the Huang–Rhys coupling parameter $S = \lambda_{internal}/(\hbar\omega)$. The large broadening and redshifting of the surface band arises from Franck–Condon progressions due to LO phonons (quantum mode) being strongly coupled to the surface state (Figure 3a). This approach has been validated by us in detail in model II–VI NCs.[12] Recently a similar

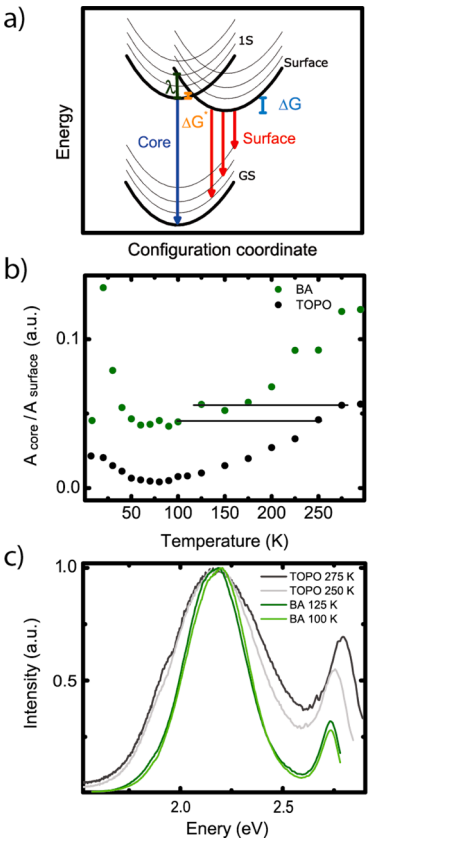

Figure 3. (a) Cartoon of our model. λ refers to the reorganization energy, ΔG^* is the activation barrier to the surface, and ΔG refers to the energy gap between the first excitonic state and the surface. (b) The ratio of integrated lineshapes of the core PL and the surface PL bands, plotted against temperature. The lines connect temperature pairs at which the PL ratio is equal for differently passivated nanocrystal. (c) Spectra for which the ratios of core to surface radiation are the same. Spectra are normalized in intensity and energy to account for the temperature dependent energy of the PL.

Marcus–Jortner approach has been used to describe metalloprotein ET.[25] The couplings to the relevant phonon modes have also been investigated in detail by us using femtosecond pump/probe spectroscopy and resonance Raman spectroscopy.[26–28]

This model is the basis for explaining the different radiative trends for differently passivated NCs shown in Figure 2. The data was fitted to said model and the fits are displayed in Figure 2c,d. The fits indicate that the model can suitably account for the complex temperature dependence of the spectra for both bands for both ligand systems. From our model we calculated the free energy differences ΔG, activation energies ΔG^*, and couplings (S, λ_{medium}) to the relevant modes for both ligand passivations (see Table 1). The main difference between the two ligand passivations is the reorganization energy for the classical mode (λ_{medium}) which corresponds to the low-frequency phonon modes of the ligands and bath, while the coupling along the quantum mode (S) is only marginally affected.[24]

TABLE 1. Calculated Variables for the Two Different Ligand Passivations[a]

	TOPO	BA
λ	96 meV	9 meV
S	19.5	20.1
ΔG	54 meV	72 meV
ΔG^*	5 meV	110 meV

[a] λ = displacement along the classical coordinate, S = Huang-Rhys parameter, ΔG = energy difference of the excitonic to the surface state, ΔG^* = activation barrier from the excitonic to the surface state.

Since the coupling to the classical mode refers to the coupling to the bath, it seems highly intuitive that changing between ligands with different chemical and steric attributes would mainly affect the coupling to the external medium. The ligands *N*-butylamine and TOPO produce substantially different chemical environments at the surface of the nanocrystal which physically translate into different energy requirements (*i.e.*, reorganization energies) to transition between the core and the surface state at a fixed configuration.

Our results indicate that the medium reorganization energy for TOPO is substantially greater than that for butylamine. Such a result is qualitatively consistent with theoretical predictions. Marcus originally invoked dielectric continuum theory to model outer sphere reorganization energy.[29] In this theory, the reorganization energy is proportional to outer sphere polarization (dielectric constant).[30,31] In our experiment, the bonds of TOPO near the surface of the NCs are substantially more polar than those for butylamine, which is expected to result in a much larger reorganization energy. Additionally, reorganization energy is proportional to the work required to reorient permanent dipoles in the outer sphere medium.[32] TOPO, as a bulky multicarbon chain molecule, requires more energy to reorient its dipoles than the quasi one-dimensional butylamine.

To the best of our knowledge, apart from our previous work only one group has measured reorganization energies for ET to nanocrystal surface states. The values of reorganization energy found by the Scholes Group are consistent with those obtained in this experiment.[33] The activation energy (ΔG^*) is inversely proportional to the coupling to the classical mode and is also hugely affected by the choice of passivating ligands. Finally, the energy gaps between the first excitonic and the surface state are slightly different (22 meV) for the different passivation cases. This can be explained by the fact that different ligands create different potentials for charge carriers on the NC surface. DFT calculations have shown that average binding energies for amine and phosphine oxide ligands are different, but on the same order of magnitude.[13]

From Figure 2 it can be seen that there are three distinct temperature domains, with different ratios of the two radiative pathways, which can be easily explained using our model. At high temperatures (~300 K to ~100 K) for TOPO-capped dots there is enough thermal energy for carriers to overcome the energy barrier (5 meV) from the band edge exciton to the surface state, as well as back transfer. Hence both core and surface radiation are present in this temperature range. Since the surface state is lower in energy (54 meV) the majority of carriers emit from the surface into the ground state. In the midtemperature regime (from ~100 K to ~70 K) there is still enough thermal energy (5 meV) for the forward charge transfer (CT) but not the reverse. In this case the core PL band drops to the noise level. In the cold temperature regime (<70 K) the forward CT reaction does not take place with efficiency due to the energy barrier (5 meV). This leads to re-emergence of detectable core emission, which in the midtemperature regime was not present.

In the case of the butylamine capped NCs, the main difference is that the core PL at all temperature relative to the surface radiation is more intense than in the TOPO case. Additionally the core PL never vanishes. Since the energy barrier is much higher than that in the TOPO case (110 meV vs 5 meV), a majority of carriers do not overcome the barrier at any temperature and the surface radiation is more a result of carriers tunneling from the band edge exciton to the surface state. However, the large energy difference of the two states (72 meV) makes tunneling back to the band edge excitonic state improbable.

On the basis of the similarities of the absorption spectra and core PL spectra, in conjunction with the success of the ET model in reproducing the functional forms of the PL response, one is poised to glean insight into how the surface may be controlled for key applications thereby enabling rational implementation of these NC systems into optoelectronic devices such as LEDs and displays. The PL spectra in Figure 2a,b would suggest in the prevailing deep trap picture that the TOPO passivated NCs merely have more surface defects than their amine counterparts. If this were the case, indeed it would indeed be difficult to rationally control these systems by suitable ligand systems. However, our simple model suggests a very simple way to reconcile the clear difference in the room temperature PL spectra. We propose that the effect of the ligand is merely to shift the thermodynamic equilibria rather than causing any selective or chemically specific "degradation" of the surface.

To further explore this idea, we address the relative intensities of each system in Figure 3. In both systems, the amount of core PL is a small fraction of the total PL (1−10%). Both systems also follow a similar functional form with some critical temperature at which there is a minimum in the relative core PL. We recently reported similar behavior in a family of II−VI NCs of a range of sizes.[12] Within this scheme, the idea is that changing

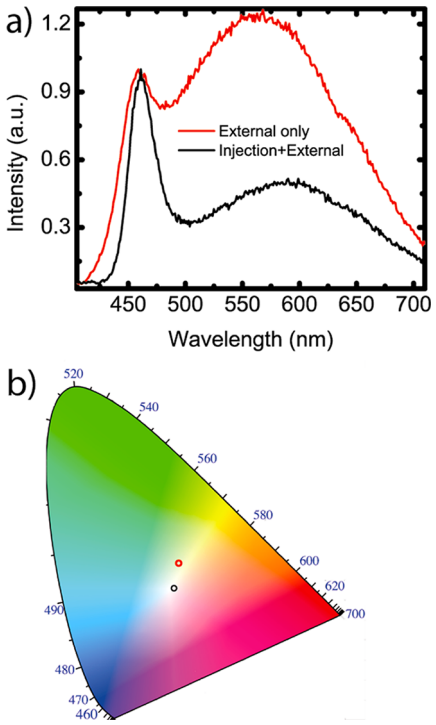

Figure 4. Synthetic control of PL spectra and color rendering capacity. (a) Normalized PL spectra of two NC batches using different cooling techniques. (b) Commission Internationale de l'Éclairage (CIE) coordinates for the different spectra. The externally cooled reaction yielded NCs with CIE coordinates of $x = 0.356$, $y = 0.398$. The externally+injection cooled reaction yielded NCs with coordinates of $x = 0.340$, $y = 0.335$, which equates to a perception of white light to the human eye.

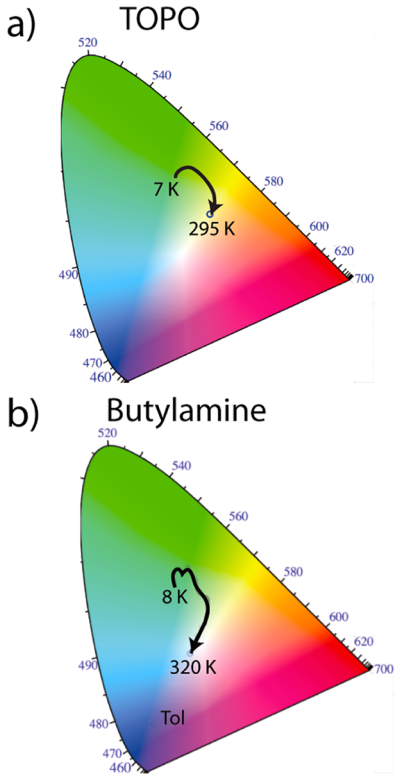

Figure 5. Thermodynamic control of PL spectra and color rendering capacity CIE diagrams for different temperatures. The arrows mark the change of color from cryogenic to room temperature. (b) The color of butylamine passivated NCs at room temperature in the blue/violet color region in addition to the color trajectory.

the surface ligands merely controls the position of the surface state in the relevant configuration coordinate diagram. In this picture, the only difference between the two systems as reflected in their PL spectra is the population equilibrium which is governed by the energy barrier differences which are the quantities that are chemically controllable by ligand exchange.

Indeed one finds tie lines which connect the relative PL intensities of the TOPO system to the amine system at some different temperature, Figure 3b. Figure 3c shows the PL spectra of the two systems at different temperatures. At room temperature, one might mistakenly conclude that the TOPO system has a more defect laden surface than the amine system due to a much more prominent surface band. Essentially, the TOPO system near room temperature is spectrally the same as the amine system at low temperature as dictated by equivalent population distributions at the dissimilar temperatures. The PL spectra would be still more similar were thermal broadening effects taken into account.[34]

In the past ultrasmall CdSe NCs have been thought of as being fundamentally different from "normal-sized" NCs.[21,35] Because most of the atoms are on the surface of the NC it has been suggested to treat these NCs as large molecules. Our results show that the PL of ultrasmall NCs can be explained by the same semiclassical electron transfer model used for NCs of bigger sizes. This strongly suggests that ultrasmall NCs are merely a subset of normal NCs. These small NCs are merely a limit to semiconductor nanocrystals in which the surface area is to be maximized for some application—white light emission in this case.

Figure 4 a shows the PL spectra of two TOPO-passivated nanocrystal samples synthesized under slightly different conditions. The only difference in the two methods was how the reaction was terminated using cooling. One reaction was cooled by submerging the reaction flask in water (external cooling only method) to quench the reaction, whereas the other reaction was quenched by external cooling and simultaneously injecting 3 mL of nonanoic acid (injection+external cooling method). The latter cooling technique produces a spectrum with a more defined core and surface peak. One possible explanation for this difference is a smaller size distribution of the NCs as this technique employs a more uniform cooling. When a comparison is made of the first absorption features of different NC batches synthesized employing both cooling techniques, the fwhm of the first absorption feature of the NCs cooled with the injection+external method is smaller. This indicates a smaller size distribution.[36] Figure 4b shows

the corresponding CIE coordinates. As can be seen from the figure, the more defined spectrum creates a light that is perceived as very white.

In previous publications the core emission has been described as biasing the white light emission to a certain color.[2] From Figure 4 it can clearly be seen that an adequate mixture of core and surface emission gives a well-balanced white light. This means that to generate high quality white light emitting NCs both radiative pathways have to be understood and taken into consideration.

In light of the capacity to rationally control the relative populations of emitting states, the core and the surface of the NCs, we finally explore the thermodynamic control of the CIE coordinates. Since the spectra are highly temperature dependent, the perceived emission color of the NCs can be varied with temperature. Temperature dependence of the CIE coordinates is pertinent to real applications of NC white light emitters, since different devices would work differently in distinct temperature regimes. Figure 5 shows the thermodynamic control of the color rendering of differently passivated NCs. The temperature dependence of the effective emission color of the samples is a result of two distinct processes. The primary cause is the changing ratio of core to surface emission with temperature. The secondary process is the blue-shifting of the PL with decreasing temperature.[34] This effect shows that apart from chemical control, the CIE color rendering of a sample can be thermodynamically controlled.

CONCLUSION

We synthesized small TOPO-capped CdSe NCs that emit white light spectra and performed a ligand exchange with butylamine which shifted the emission from a surface dominated to a core dominated spectrum. Using temperature dependent PL we determined that there is a free energy change of the surface state upon ligand exchange and that the ratio of core to surface radiation can be controlled with temperature. We showed that all observations from room temperature to cryogenic temperatures could be explained using a Marcus-Jortner electron transfer model. Finally we showed that good white light emitting NCs needs a well-balanced ratio of core and surface radiation. These results demonstrate that the emission of small white light emitting CdSe NCs can be understood the same way as the emission of normal-sized CdSe nanostructures and that surface chemistry and thermal energy can be utilized to rationally design single white light NC emitters.

METHODS

Synthetic. Trioctylphosphine oxide (TOPO, 99% Aldrich), cadmium oxide (CdO, 99.99% Sigma Aldrich), selenium powder (Se, 99.5%, 100-mesh Aldrich), trioctylphosphine (TOP, 97% Aldrich), butylamine (BA, 99.5% Sigma Aldrich), and tetradecylphosphonic acid (TDPA, 99% PCI) were used as received. The injection solution was made by dissolving 0.3560 g of Se in 2 g of TOP under argon.

The synthesis is adopted from Peng.[11] Amounts of 0.523 g of CdO, 3.96 g of TOPO, and 0.211 g of TDPA were transferred to a 3-neck round-bottom flask which then was evacuated, and argon was introduced. Under stirring the flask was heated to 300 °C, and the sides of the flask were rinsed down with ~2 g of TOP once the temperature was reached. The flask was heated to 325 °C until the solution was clear and the heating mantle was removed and replaced with an empty basin. At 310 °C the Se/TOP solution was swiftly injected and after 2−5 s the reaction was cooled by simultaneously injecting 3 mL of nonanoic acid and flooding the basin with water. Once the reaction had cooled to 80 °C ~5 mL of nonanoic acid was added. The reaction mixture was transferred to a centrifuge tube and was fractionally centrifuged by adding ~5 mL of MeOH and centrifuging at 7000 rpm for 20 min to remove larger NCs. The mixture was decanted into a second centrifuge tube and ~40 mL of MeOH was added. After 20 min at 7000 rpm the centrifuge tube was drained and the NCs were dissolved in toluene.

For the ligand exchange ~3 mL of nanocrystal/toluene solution were transferred to a 3-neck round-bottom flask which was put under vacuum until all toluene had evaporated, and the flask was consequently filed with argon. The neat NCs were dissolved in ~3 mL of butylamine, and the solution was stirred for 2 days. As in previous research a full ligand exchange is not assumed, rather it is assumed that a large majority of ligand sites are exchanged[16,30]

Experiment. The absorption spectra were taken on a Cary 5000 UV−vis spectrometer. A Fluoromax 2 PL spectrometer was used to acquire PL spectra. All room temperature spectra were taken in toluene. The NCs were transferred to a polystyrene solution in toluene and drop cast in a Petri dish. After about 2 days of drying, the film was transferred into a flow cryostat. To find the temperature-dependent first absorption feature, absorption spectra at selected temperatures were obtained, and the energies of the temperature-dependent absorption feature were recorded and fit to the following equation $E_g(T) = E_g(0) - (\alpha T^2)/(T+\beta)$ (the Varshni model), where $E_g(0)$, α, and β are material constants.[34] The sample was excited at the energy of the first absorption feature at the respective temperature.

Conflict of Interest: The authors declare no competing financial interest.

Supporting Information Available: Details of modeling. This material is available free of charge *via* the Internet at http://pubs.acs.org.

Acknowledgment. We would like to thank Jun Yang & Frank Wise, and also Ross Dorner & Vlatko Vedral for helpful discussions. We would like to express our gratitude to Richard Rossi and Jean-Philippe Guay for their technical support. Financial support from the CFI, NSERC, FQRNT, and McGill University is acknowledged. We thank the McGill University Center for Self-Assembled Chemical Structures for use of their facilities.

REFERENCES AND NOTES

1. Provoost, R.; Gotzeler, M. A Global Transition to Efficient Lighting. http://www.unep.org/climatechange/Portals/5/documents/global_transition_efficient_lighting.pdf.
2. Bowers, M. J.; McBride, J. R.; Rosenthal, S. J. White-Light Emission from Magic-Sized Cadmium Selenide Nanocrystals. *J. Am. Chem. Soc.* **2005**, *127*, 15378–15379.
3. Rogach, Andrey L.; Gaponik, N.; Lupton, John M.; Bertoni, C.; Gallardo, Diego E.; Dunn, S.; Li Pira, N.; Paderi, M.; Repetto, P.; Romanov; *et al*. Light-Emitting Diodes with Semiconductor Nanocrystals. *Angew. Chem., Int. Ed.* **2008**, *47*, 6538–6549.

4. Sapra, S.; Mayilo, S.; Klar, T. A.; Rogach, A. L.; Feldmann, J. Bright White-Light Emission from Semiconductor Nanocrystals: by Chance and by Design. *Adv. Mater.* **2007**, *19*, 569–572.
5. Talapin, D. V.; Rogach, A. L.; Kornowski, A.; Haase, M.; Weller, H. Highly Luminescent Monodisperse CdSe and CdSe/ZnS Nanocrystals Synthesized in a Hexadecylamine—Trioctylphosphine Oxide—Trioctylphosphine Mixture. *Nano Lett.* **2001**, *1*, 207–211.
6. Coe, S.; Woo, W.-K.; Bawendi, M.; Bulovic, V. Electroluminescence from Single Monolayers of Nanocrystals in Molecular Organic Devices. *Nature* **2002**, *420*, 800–803.
7. Achermann, M.; Petruska, M. A.; Koleske, D. D.; Crawford, M. H.; Klimov, V. I. Nanocrystal-Based Light-Emitting Diodes Utilizing High-Efficiency Nonradiative Energy Transfer for Color Conversion. *Nano Lett.* **2006**, *6*, 1396–1400.
8. Tessler, N.; Medvedev, V.; Kazes, M.; Kan, S.; Banin, U. Efficient Near-Infrared Polymer Nanocrystal Light-Emitting Diodes. *Science* **2002**, *295*, 1506–1508.
9. Lee, J.; Sundar, V. C.; Heine, J. R.; Bawendi, M. G.; Jensen, K. F. Full Color Emission from II—VI Semiconductor Quantum Dot—Polymer Composites. *Adv. Mater.* **2000**, *12*, 1102–1105.
10. Mueller, A. H.; Petruska, M. A.; Achermann, M.; Werder, D. J.; Akhadov, E. A.; Koleske, D. D.; Hoffbauer, M. A.; Klimov, V. I. Multicolor Light-Emitting Diodes Based on Semiconductor Nanocrystals Encapsulated in GaN Charge Injection Layers. *Nano Lett.* **2005**, *5*, 1039–1044.
11. Peng, Z. A.; Peng, X. Formation of High-Quality CdTe, CdSe, and CdS Nanocrystals Using CdO as Precursor. *J. Am. Chem. Soc.* **2001**, *123*, 183–184.
12. Mooney, J.; Krause, M. M.; Saari, J. I.; Kambhampati, P. Challenge to the Deep-Trap Model of the Surface in Semiconductor Nanocrystals. *Phys. Rev. B* **2013**, *87*, 081201.
13. Mooney, J.; Krause, M. M.; Saari, J. I.; Kambhampati, P. A Microscopic Picture of Surface Charge Trapping in Semiconductor Nanocrystals. *J. Chem. Phys.* **2013**, *138*, 204705.
14. Yu, W. W.; Qu, L.; Guo, W.; Peng, X. Experimental Determination of the Extinction Coefficient of CdTe, CdSe, and CdS Nanocrystals. *Chem. Mater.* **2003**, *15*, 2854–2860.
15. Murray, C. B.; Norris, D. J.; Bawendi, M. G. Synthesis and Characterization of Nearly Monodisperse CdE (E = Sulfur, Selenium, Tellurium) Semiconductor Nanocrystallites. *J. Am. Chem. Soc.* **1993**, *115*, 8706–8715.
16. Kuno, M.; Lee, J. K.; Dabbousi, B. O.; Mikulec, F. V.; Bawendi, M. G. The Band Edge Luminescence of Surface Modified CdSe Nanocrystallites: Probing the Luminescing State. *J. Chem. Phys.* **1997**, *106*, 9869–9882.
17. Garrett, M. D.; Bowers, M. J.; McBride, J. R.; Orndorff, R. L.; Pennycook, S. J.; Rosenthal, S. J. Band Edge Dynamics in CdSe Nanocrystals Observed by Ultrafast Fluorescence Upconversion. *J. Phys. Chem. C* **2008**, *112*, 436–442.
18. Underwood, D. F.; Kippeny, T.; Rosenthal, S. J. Ultrafast Carrier Dynamics in CdSe Nanocrystals Determined by Femtosecond Fluorescence Upconversion Spectroscopy. *J. Phys. Chem. B* **2001**, *105*, 436–443.
19. Kalyuzhny, G.; Murray, R. W. Ligand Effects on Optical Properties of CdSe Nanocrystals. *J. Phys. Chem. B* **2005**, *109*, 7012–7021.
20. Hines, M. A.; Guyot-Sionnest, P. Bright UV-Blue Luminescent Colloidal ZnSe Nanocrystals. *J. Phys. Chem. B* **1998**, *102*, 3655–3657.
21. Landes, C. F.; Braun, M.; El-Sayed, M. A. On the Nanoparticle to Molecular Size Transition: Fluorescence Quenching Studies. *J. Phys. Chem. B* **2001**, *105*, 10554–10558.
22. Jones, M.; Nedeljkovic, J.; Ellingson, R. J.; Nozik, A. J.; Rumbles, G. Photoenhancement of Luminescence in Colloidal CdSe Quantum Dot Solutions. *J. Phys. Chem. B* **2003**, *107*, 11346–11352.
23. Haesselbarth, A.; Eychmüller, A.; Weller, H. Detection of Shallow Electron Traps in Quantum Sized Cadmium Sulfide by Fluorescence Quenching Experiments. *Chem. Phys. Lett.* **1993**, *203*, 271–276.
24. Jortner, J. Temperature Dependent Activation Energy for Electron Transfer between Biological Molecules. *J. Chem. Phys.* **1976**, *64*, 4860.
25. Dorner, R.; Goold, J.; Heaney, L.; Farrow, T.; Vedral, V. Effects of Quantum Coherence in Metalloprotein Electron Transfer. *Phys. Rev. E* **2012**, *86*, 031922.
26. Kambhampati, P. Unraveling the Structure and Dynamics of Excitons in Semiconductor Quantum Dots. *Acc. Chem. Res.* **2011**, *44*, 1–13.
27. Kambhampati, P. Hot Exciton Relaxation Dynamics in Semiconductor Quantum Dots: Radiationless Transitions on the Nanoscale. *J. Phys. Chem. C* **2011**, *115*, 22089–22109.
28. Sagar, D. M.; Cooney, R. R.; Sewall, S. L.; Dias, E. A.; Barsan, M. M.; Butler, I. S.; Kambhampati, P. Size Dependent, State-Resolved Studies of Exciton-Phonon Couplings in Strongly Confined Semiconductor Quantum Dots. *Phys. Rev. B* **2008**, *77*, 235321–235314.
29. Marcus, R. A. On the Theory of Electron-Transfer Reactions. VI. Unified Treatment for Homogeneous and Electrode Reactions. *J. Chem. Phys.* **1965**, *43*, 679–701.
30. Gupta, S.; Matyushov, D. V. Effects of Solvent and Solute Polarizability on the Reorganization Energy of Electron Transfer. *J. Phys. Chem. A* **2004**, *108*, 2087–2096.
31. Matyushov, D. V. Solvent Reorganization Energy of Electron-Transfer Reactions in Polar Solvents. *J. Chem. Phys.* **2004**, *120*, 7532–7556.
32. Matyushov, D. V. Reorganization Energy of Electron Transfer in Polar Liquids. Dependence on Reactant Size, Temperature and Pressure. *Chem. Phys.* **1993**, *174*, 199–218.
33. Jones, M.; Lo, S. S.; Scholes, G. D. Signatures of Exciton Dynamics and Carrier Trapping in the Time-Resolved Photoluminescence of Colloidal CdSe Nanocrystals. *J. Phys. Chem. C* **2009**, *113*, 18632–18642.
34. Valerini, D.; Creti, A.; Lomascolo, M.; Manna, L.; Cingolani, R.; Anni, M. Temperature Dependence of the Photoluminescence Properties of Colloidal CdSe/ZnS Core/Shell Quantum Dots Embedded in a Polystyrene Matrix. *Phys. Rev. B* **2005**, *71*, 2354091–2354096.
35. McBride, J. R.; Dukes, A. D., 3rd; Schreuder, M. A.; Rosenthal, S. J. On Ultrasmall Nanocrystals. *Chem. Phys. Lett.* **2010**, *498*, 1–9.
36. Salvador, M. R.; Graham, M. W.; Scholes, G. D. Exciton-Phonon Coupling and Disorder in the Excited States of CdSe Colloidal Quantum Dots. *J. Chem. Phys.* **2006**, *125*, 184709.